Check for updates

Journal of Applied Toxicology

WILEY

Journal of AppliedToxicology

RESEARCH ARTICLE

Exposure Risks of Trans-Perfluoro (4-Methyl-2-Pentene) Byproduct in $C_6F_{12}O$ Fire Suppressants: Toxicological Mechanisms and Implications

Biao Zhou[1] | Muying Ge[1] | Kai Wang[1] | Peiyao Chen[2] | Jin He[3] | Haiting Wu[1] | Wanyu Yang[4] | Hongru Zhou[1]

[1]School of Emergency Management and Safety Engineering, China University of Mining and Technology, Beijing, China | [2]Tianjin Fire Science Technology Research Institute of MEM, Tianjin, China | [3]Sichuan Fire Research Institute of MEM, Chengdu, Sichuan, China | [4]Department of Architecture, Faculty of Engineering, University of Tokyo, Tokyo, Japan

Correspondence: Biao Zhou (zhoubiao1088@cumtb.edu.cn)

Received: 14 May 2025 | **Revised:** 13 July 2025 | **Accepted:** 15 July 2025

Funding: This work was supported by the Beijing Municipal Science and Technology Project (Z231100003823022), the Ordos Key Research and Development Program (YF20240026), the Beijing Nova Program (202504841008), the Tianjin Natural Science Foundation Project (22JCZDJC00880), the Key-Area Research and Development Program of Guangdong Province (2024B1111080002), and the Fundamental Research Funds for the Central Universities (2025ZKPYAQ03).

Keywords: histopathological analysis | IL-1β levels | oral toxicity | perfluoro (4-methyl-2-pentene)

ABSTRACT

$C_6F_{12}O$ fire agent is widely used in various fire extinguishing scenarios due to its excellent properties. The most abundant byproduct in $C_6F_{12}O$ fire extinguishing agent is perfluoro (4-methyl-2-pentene) (C_6F_{12}). Currently, there is a lack of reports on the toxic mechanisms of trans-C_6F_{12}. This study investigated the acute oral toxicity of trans-C_6F_{12} in rats, the damage mechanisms to major organs, and evaluated the inflammatory status of various organs. The experimental design comprised four treatment groups: a control group, a low-dose group (250 mg/kg), a medium-dose group (500 mg/kg), and a high-dose group (750 mg/kg), encompassing the range from sublethal to lethal concentrations. The median lethal dose (LD50) for trans-C_6F_{12} revealed its mild acute toxicity, with male rats exhibiting significantly higher sensitivity. Clinical observations showed that trans-C_6F_{12} oral exposure caused symptoms such as lethargy and reduced appetite. Pathological analysis revealed that trans-C_6F_{12} primarily caused significant damage to the respiratory and urinary systems, particularly in lung and kidney tissues. Additionally, moderate damage was observed in the liver, heart, and spleen, whereas only mild pathological changes were detected in the classical hippocampus, and no effects were observed in ocular tissues. Further analysis of the inflammatory cytokine IL-1β levels showed that lung and kidney tissues were more sensitive to the toxicity of trans-C_6F_{12}, exhibiting significant inflammatory responses. In contrast, the inflammatory responses in other organs were relatively weak. This study revealed the toxicity of trans-C_6F_{12} and its toxicological mechanisms, providing important references for the safe use of $C_6F_{12}O$ fire extinguishing agent.

1 | Introduction

Because Halon 1301 (CF_3Br) was banned under the Montreal Protocol, researchers have been striving to find more environmentally friendly and efficient fire extinguishing agents (Babushok et al. 2022). $C_6F_{12}O$ fire extinguishing agent ($C_6F_{12}O$, CAS No. 756-13-8, 99%) possesses excellent properties, including low corrosivity, low toxicity, low fire extinguishing volume fraction, zero ozone depletion potential (ODP = 0), environmental friendliness (GWP = 1), and ease of storage at room temperature (Pagliaro and Linteris 2017; Xing, Lu, Yang, et al. 2022). It has been approved by UL and FM in the United States (Han

© 2025 John Wiley & Sons Ltd.

et al. 2023). $C_6F_{12}O$ fire extinguishing agent is predominantly composed of $C_6F_{12}O$, accounting for approximately 99% by mass. The most abundant byproduct in this fire extinguishing agent is C_6F_{12}, which is primarily generated during the synthesis of $C_6F_{12}O$. On the one hand, $C_6F_{12}O$ fire extinguishing agent is primarily used for total flooding fire suppression, requiring a large amount. Therefore, the potential health effects of C_6F_{12} merit heightened concern as it constitutes the predominant byproduct of $C_6F_{12}O$ fire extinguishing agent. As personnel involved in firefighting and rescue operations will inevitably come into contact with the extinguishing agent, understanding the toxicity risks of C_6F_{12} is necessary. On the other hand, the toxicity of byproducts also partially determines compliance with application regulations, as well as the implementation of appropriate industrial hygiene or safety measures. In addition, a study has demonstrated the primary decomposition kinetics of C_6F_{12} and its interaction with flames. The results indicate that the flame suppression effect of C_6F_{12} is comparable to $C_6F_{12}O$. Therefore, C_6F_{12} also exhibits considerable potential as a fire extinguishing agent (X. Wang et al. 2023). This warrants significant research attention on C_6F_{12} as a potential fire-extinguishing agent. Consequently, assessing the toxicity and application risks of C_6F_{12} is important and urgent.

Currently, significant research efforts have been devoted to the $C_6F_{12}O$ fire extinguishing agent. First, extensive investigations have been conducted on its thermophysical properties, including vapor pressure (McLinden et al. 2015), temperature-dependent viscosity (Cui et al. 2018; Wen et al. 2017), and thermal conductivity (Perkins et al. 2018). Second, studies have focused on the fire-extinguishing performance of $C_6F_{12}O$ (Pagliaro and Linteris 2017; Liu et al. 2019; S. S. Tian et al. 2024) and suppression effects on lithium-ion battery fires (K. Wang et al. 2025; Huang et al. 2025), hydrogen jet flames (Fan et al. 2023), H_2-CH_4-air mixture flames (N. Luo et al. 2025), deflagration of hydrogen compressed natural gas (J. Wang et al. 2025), coaxial n-heptane flame (Xing, Lu, Tao, et al. 2025), and ethanol-gasoline vapor explosion (Pan et al. 2021), and studies have also focused on the minimum extinguishing concentration (Han et al. 2023). Additionally, some studies have been conducted on the composition of its pyrolysis products (Li et al. 2019; Zeng et al. 2019; Zhang, Tian, et al. 2017) and associated pyrolysis mechanisms (Xing, Cheng, Lu, et al. 2021). Previous studies have shown that its main pyrolysis products include CF_4, C_2F_6, C_3F_8, C_3F_6, C_4F_{10}, and C_5F_{12} (Xing, Cheng, Lu, et al. 2021). In terms of toxicity research, well-established toxicity assessment protocols and mechanisms are currently available (Wallig et al. 2017). Previous studies have also conducted extensive research on fluoride toxicity (Johnston and Strobel 2020). Some research has primarily examined the corrosiveness and toxicity of $C_6F_{12}O$'s pyrolysis gas (Xing, Lu, Yang, et al. 2022; Zhang, Li, et al. 2017). Research institutions have shown that the median lethal concentration (LC50) for $C_6F_{12}O$ is 1227 mg/L (rat, inhalation, 4 h), and the time-weighted average (TWA) occupational exposure limit is 150 ppm (1940 mg/m^3). Additionally, studies determined that the LC50 of HF is 1276 ppm (rat, inhalation, 1 h) and 342 ppm (mouse, inhalation, 1 h). However, research on C_6F_{12} has primarily focused on its synthesis and isomerization, with limited reports addressing its safety and application risks. Given both its proportion in the $C_6F_{12}O$ fire extinguishing agent and inherent fire suppression potential, elucidating the toxicity profile of C_6F_{12} carries significant practical implications. Such research would not only provide critical safety data for the $C_6F_{12}O$ fire extinguishing agent but also establish an essential foundation for developing next-generation fluorinated fire suppression technologies.

This paper focuses on elucidating the toxicity mechanisms of trans-C_6F_{12} (perfluoro [4-methyl-2-pentene], CAS No. 2070-70-4) following oral exposure, addressing the current knowledge gap in its toxicological profile. Additionally, alterations in vital signs of rats after gavage administration were investigated. The preliminary experimental design was established according to the "OECD Guideline for Testing of Chemicals-Acute Oral Toxicity-Acute Toxic Class Method" (OECD 423, December 17, 2001) (OECD 2001). The preliminary study employed an initial dose of 300 mg/kg, with the high-dose group set at 2000 mg/kg. Based on preliminary findings, the formal experiment comprised: a control group administered equivalent-volume corn oil by gavage; low dose (250 mg/kg); medium dose (500 mg/kg); and high dose (750 mg/kg) groups. This dose-range design, spanning from sublethal to lethal concentrations, facilitates a comprehensive evaluation of the toxicological mechanisms of trans-C_6F_{12} in rats. This study reveals the damage caused by trans-C_6F_{12} to major organs in rats through pathological section analysis. And the inflammatory status of various organs was evaluated by analyzing the expression levels of proinflammatory cytokines. The findings not only elucidate the toxic mechanisms of trans-C_6F_{12} but also provide important references for the safety protection of rescue personnel.

2 | Materials and Methods

2.1 | Test Item

It is reported that C_6F_{12} is the most abundant byproduct in the $C_6F_{12}O$ fire extinguishing agent, based on chromatogram peak order. The chromatogram of the $C_6F_{12}O$ fire extinguishing agent is shown in Figure 1a. Trans-C_6F_{12} (perfluoro [4-methyl-2-pentene], CAS No. 2070-70-4) was specifically investigated as the research subject in this study, as shown in Figure 1b. Trans-C_6F_{12}, with a boiling point of 49°C and a density of 1.59 g/cm^3, is generated as a byproduct during the synthesis of $C_6F_{12}O$. The trans-C_6F_{12} and $C_6F_{12}O$ used in this study were purchased from Zhejiang Noah Fluorochemical Co. Ltd.

2.2 | Animals

This study utilized specific pathogen-free (SPF) healthy Sprague–Dawley (SD) rats. For the preliminary experiment, six 8-week-old female rats were used, whereas the formal experiment employed forty 6- to 8-week-old rats (10 rats per group with 5 males and 5 females), all purchased from SPF (Beijing) Biotechnology Co. Ltd. (Animal Certification: No. 110324241105210061). Throughout the study, the animals were housed in cages (length × width × height: 54 × 39.5 × 20 cm). Prior to the experiment, rats underwent a 7-day acclimation period to rule out interference from adaptation stress. The housing environment was maintained at 22°C ± 3°C, humidity of 50% ± 10%, and a 12-h light/dark cycle, with free access

10991263, 0, Downloaded from https://analyticalsciencejournals.onlinelibrary.wiley.com/doi/10.1002/jat.4868 by China University Of Mining, Wiley Online Library on [29/07/2025]. See the Terms and Conditions (https://onlinelibrary.wiley.com/terms-and-conditions) on Wiley Online Library for rules of use; OA articles are governed by the applicable Creative Commons License

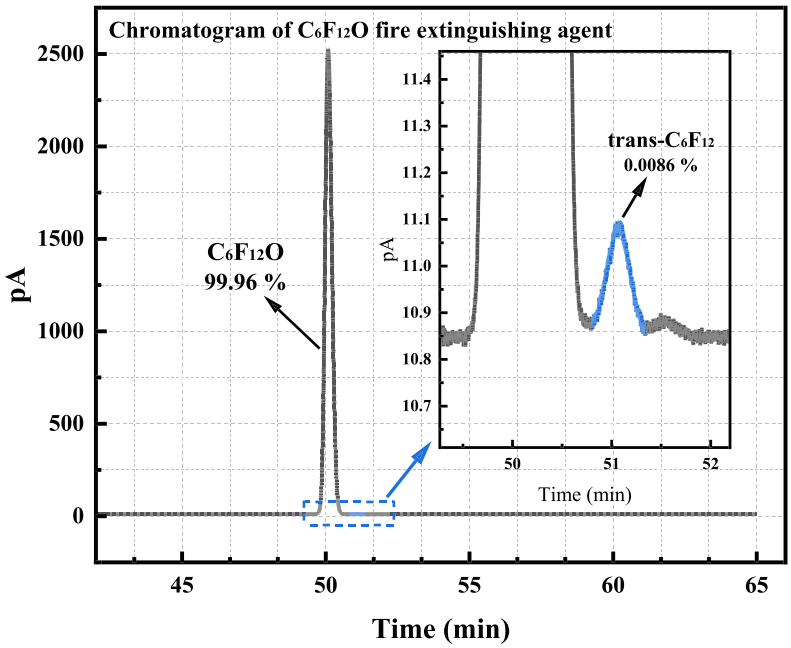

(a)

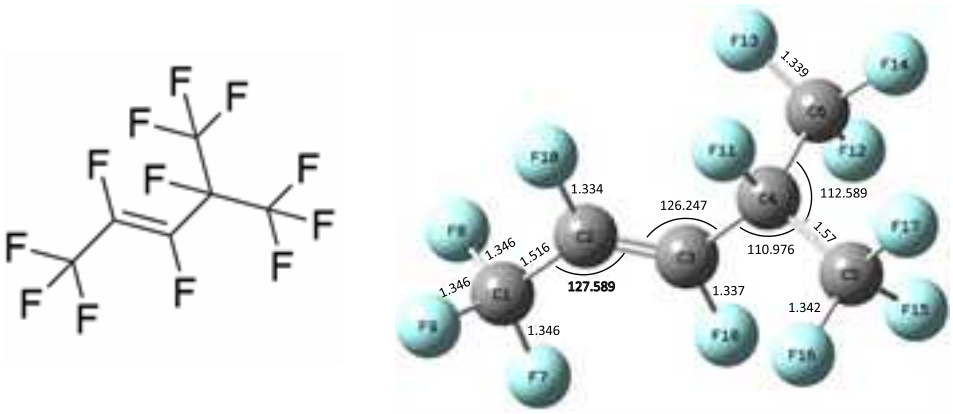

(b)

FIGURE 1 | Chromatogram of the $C_6F_{12}O$ fire extinguishing agent and C_6F_{12}. (a) Chromatogram of the $C_6F_{12}O$ fire extinguishing agent. (b) Molecular structure of trans-C_6F_{12}.

to food and water. The experimental protocol was approved by the Animal Ethical and Welfare Committee of Beijing Kewei Te Animal Technology Co. Ltd. (Ethical Approval: No. KWT-2024-0821-01), with strict adherence to the "3R" (replacement, reduction, refinement) principles for animal welfare management.

2.3 | Test Procedure

Before the experiment, the rats were fasted for 12 h, with water allowed freely. After the fasting period, the rats were weighed and numbered. Given the high boiling point of trans-C_6F_{12} (49°C), it requires maintaining the ambient temperature above 50°C to keep trans-C_6F_{12} in a constant gaseous state for rat inhalation. This would create excessively high temperatures for rat survival, thereby significantly compromising experimental results. Consequently, liquid gavage was adopted to study the substance's toxicity. The trans-C_6F_{12} was fully dissolved in corn oil at the experimental concentration and administered via gavage twice. Doses were administered at 6-h intervals to more accurately replicate the real-life situation of repeated short-term exposure to fire suppressants while preventing acute mortality due to a single high-dose administration. After the first gavage, the rats were allowed free access to food and water.

A preliminary experiment was conducted initially. The preliminary experiment was designed based on the "OECD Guideline for Testing of Chemicals-Acute Oral Toxicity-Acute Toxic Class Method" (OECD 423, December 17, 2001) (OECD 2001), with three female rats selected for each step. Based on animal welfare principles, the initial dose was set at 300 mg/kg. The concentration for the high-dose group was set at 2000 mg/kg.

The formal experiment included 10 rats per group (5 females and 5 males), with four groups: control, low-dose, medium-dose, and high-dose groups. The experimental concentrations were determined through the preliminary experiment, with the control group receiving corn oil of the same volume via

10991263, 0, Downloaded from https://analyticalsciencejournals.onlinelibrary.wiley.com/doi/10.1002/jat.4868 by China University Of Mining, Wiley Online Library on [29/07/2025]. See the Terms and Conditions (https://onlinelibrary.wiley.com/terms-and-conditions) on Wiley Online Library for rules of use; OA articles are governed by the applicable Creative Commons License

gavage; the low-dose group receiving 250 mg/kg trans-C_6F_{12} solution; the medium-dose group receiving 500 mg/kg trans-C_6F_{12} solution; and the high-dose group receiving 750 mg/kg trans-C_6F_{12} solution. The dose levels were selected to span from sublethal to lethal ranges, thereby enabling a systematic investigation of the toxicological mechanisms of trans-C_6F_{12} in rats. The specific experimental parameters are shown in Table 1.

After dosing, the rats were observed, and their behavior was recorded daily for 14 days. Key observations included survival status, food and water consumption, respiratory rate and depth, changes in fur, motor ability, presence of convulsions, eye examination indicators, gastrointestinal signs, and body weight trends. Additionally, blood samples were collected via tail vein puncture at the end of the experiment, and organ tissues were collected at the end of the experiment for correlation analysis.

Tissue samples from the liver, heart, spleen, lungs, kidneys, classical hippocampus, and eyes were used to prepare histopathological sections. The tissues were fixed with 4% paraformaldehyde, followed by routine extraction, dehydration, paraffin embedding, sectioning (4 μm thick), and HE staining. The histopathological sections were then photographed under an optical microscope (PANNORAMIC MIDI II, 3DHISTECH, Budapest, Hungary).

Immunofluorescence single labeling was performed on tissue sections (liver, heart, spleen, lungs, kidneys, and classical hippocampus). Fluorescence images were acquired at predetermined wavelengths after mounting. Quantitative analysis of IL-1β-positive areas was performed using Aipathwell software to determine the expression levels of proinflammatory cytokine. In order to further evaluate the inflammatory response and immune system effects induced by trans-C_6F_{12}, the overall experimental setup is shown in Figure 2.

TABLE 1 | Experimental conditions.

Category	No.	Dose level	Concentration (mg/kg)	Sample composition
Preexperiment	1	Low-dose group	300	3 rats (females)
	2	High-dose group	2000	3 rats (females)
Formal experiment	1	Control group	0	10 rats (5 females and 5 males)
	2	Low-dose group	250	10 rats (5 females and 5 males)
	3	Medium-dose group	500	10 rats (5 females and 5 males)
	4	High-dose group	750	10 rats (5 females and 5 males)

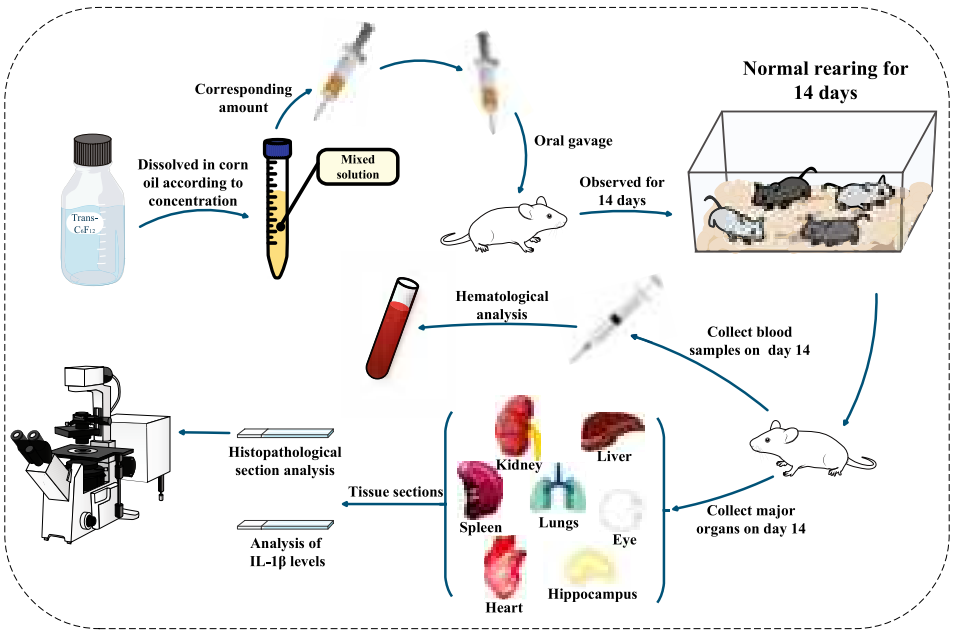

FIGURE 2 | Experimental flowchart.

10991263, 0, Downloaded from https://analyticalsciencejournals.onlinelibrary.wiley.com/doi/10.1002/jat.4868 by China University Of Mining, Wiley Online Library on [29/07/2025]. See the Terms and Conditions (https://onlinelibrary.wiley.com/terms-and-conditions) on Wiley Online Library for rules of use; OA articles are governed by the applicable Creative Commons License

2.4 | Statistical Analysis

Means and standard deviations were calculated for all quantitative measurements. One-way ANOVA was followed by the Holm–Bonferroni post hoc correction to control the family-wise error rate while maintaining pairwise comparisons between each dose group and the control. Significance was set at $p < 0.05$.

3 | Results and Discussion

3.1 | The Results of the Calibration Test

To investigate the acute oral toxicity of trans-C_6F_{12}, a preliminary oral toxicity experiment was conducted to determine the appropriate concentrations for the formal experiment. The preliminary oral toxicity experiment was established in compliance with the "OECD 423, December 17, 2001 (OECD 2001)," as illustrated in Figure 3. Trans-C_6F_{12} was fully dissolved in corn oil, and an initial dose of 300 mg/kg was prepared. The trans-C_6F_{12} solution was administered via gavage in doses corresponding to the rats' body weight. After 14 days of observation, no deaths occurred. A trans-C_6F_{12} solution with a concentration of 2000 mg/kg was then prepared and administered via gavage according to the rats' body weight. All rats died within 3 days of dosing.

Based on the results of the preliminary experiment, the formal experiment employed the following dose concentrations: low-dose (250 mg/kg), medium-dose (500 mg/kg), and high-dose (750 mg/kg) groups, to cover the sublethal-to-lethal range.

3.2 | Clinical Observations

An oral administration experiment was conducted to investigate the acute oral toxicity of trans-C_6F_{12} at different concentrations. Trans-C_6F_{12} was dissolved in corn oil to prepare solutions with concentrations of 250 mg/kg (low-dose group), 500 mg/kg (medium-dose group), and 750 mg/kg (high-dose group). The control group received the corn oil via oral gavage based on their body weight, whereas the other rats were administered corresponding doses of the trans-C_6F_{12} solution based on their body weight. The symptoms observed in rats after oral administration are summarized as follows:

After oral administration, no rats died in the low-dose group (250 mg/kg). In the medium-dose group (500 mg/kg), one female rat died on the third day and two male rats died on the fourth day postadministration, resulting in a total of three deaths. In the high-dose group (750 mg/kg), two male and two female rats died on the third day and two male rats died on the fourth day, for a total of six deaths. The specific results are presented in Table 2. Based on the experimental results,

TABLE 2 | Mortality rate of rats after trans-C_6F_{12} gavage exposure.

No.	Test condition	Mortality rate		
		Male	Female	Total
1	Control group	0/5	0/5	0/10
2	250 mg/kg	0/5	0/5	0/10
3	500 mg/kg	2/5	1/5	3/10
4	750 mg/kg	4/5	2/5	6/10

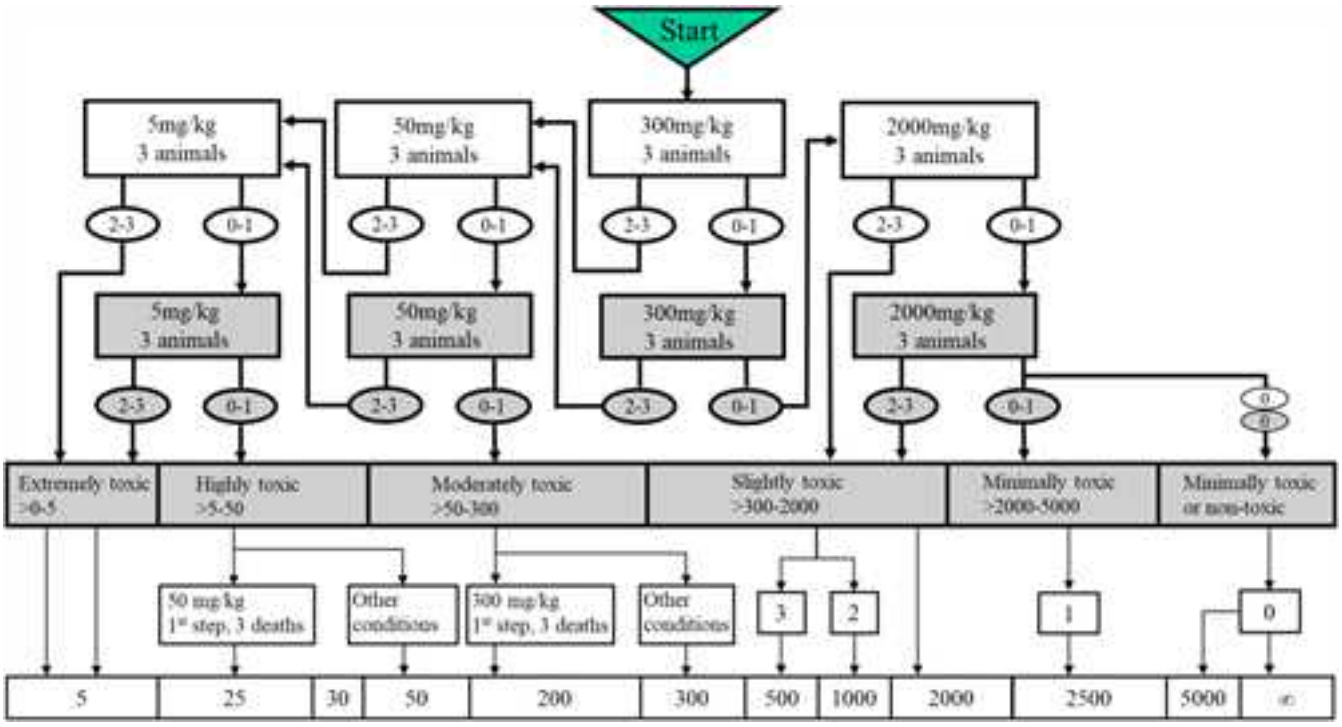

FIGURE 3 | Acute oral toxicity–acute toxic class method (OECD 2001).

10991263, 0, Downloaded from https://analyticalsciencejournals.onlinelibrary.wiley.com/doi/10.1002/jat.4868 by China University Of Mining, Wiley Online Library on [29/07/2025]. See the Terms and Conditions (https://onlinelibrary.wiley.com/terms-and-conditions) on Wiley Online Library for rules of use; OA articles are governed by the applicable Creative Commons License

the median lethal dose (LD50) of trans-C_6F_{12} was calculated using Bliss's method. The sex-specific LD50 values were determined to be 823 mg/kg for female rats and 558 mg/kg for male rats, with a combined LD50 of 655 mg/kg when sex differences were not considered. These results demonstrate that male rats exhibited greater sensitivity to trans-C_6F_{12} toxicity compared to females.

After oral exposure, the rats showed reduced food and water intake, and body weight loss was observed in all concentration groups. The rats exhibited persistent watery stools for several days. In the low-dose group, normal excretion began to recover on the third day postadministration and fully recovered by the fifth day. Recovery was observed by Day 9 in the medium-dose group and by Day 13 in the high-dose group. Therefore, all three concentrations of trans-C_6F_{12} are considered to have gastrointestinal toxicity. In terms of activity, all rats across the different concentration groups showed lethargy after oral administration, and the duration of lethargy was proportional to the concentration, as shown in Figure 4a. Additionally, stress-like behaviors were observed in all three groups when stimulated (rapid repetitive running in the cage) during the first 2 days, as shown in Figure 4b. The stress response gradually diminished. In the high-dose group, multiple rats exhibited piloerection, whereas individual rats in the other two groups also showed piloerection. Significant fur loss in the genital region and skin redness were

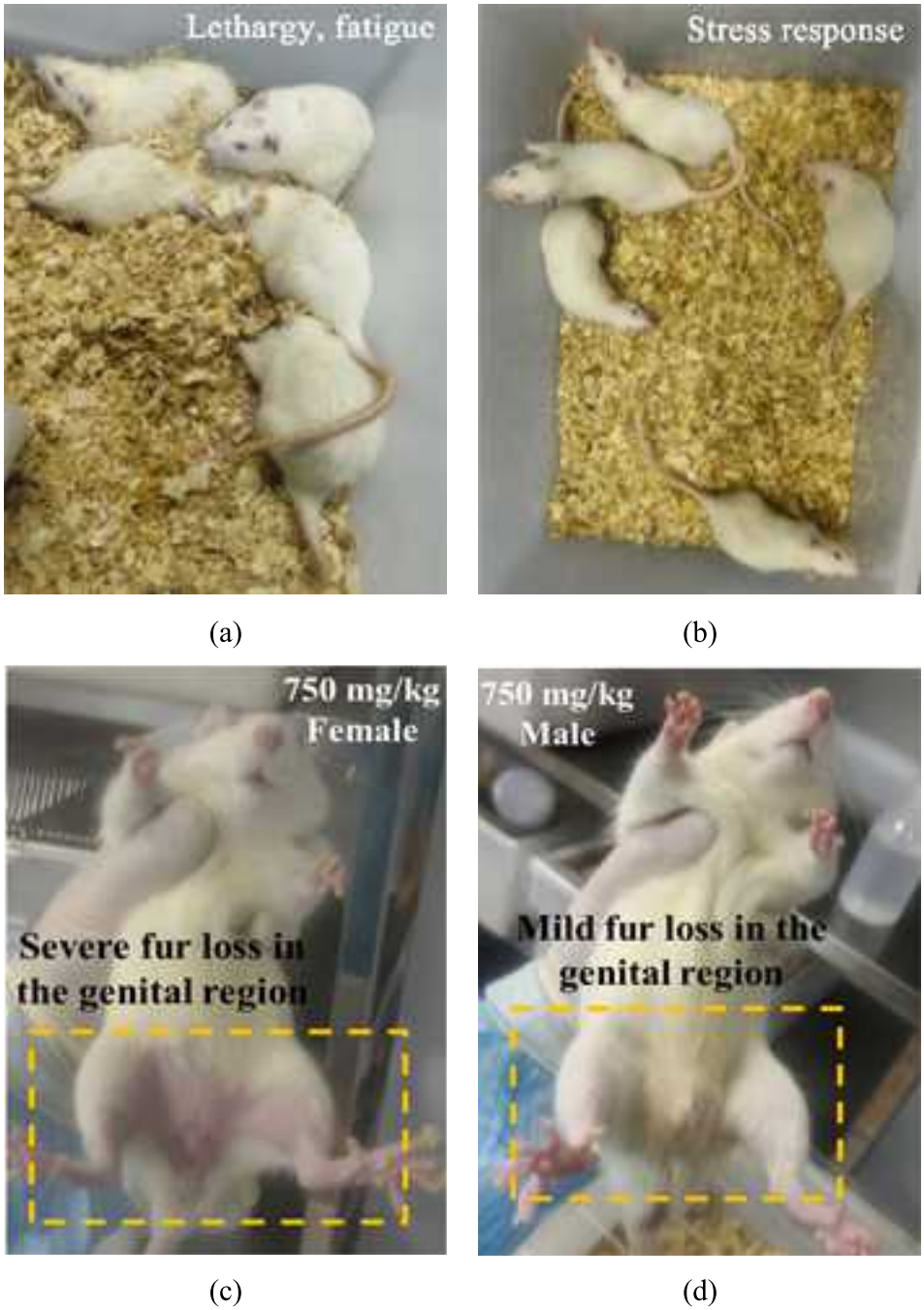

FIGURE 4 | Characterization of rats after gavage exposure. (a) Lethargy observed following gavage exposure. (b) Stress response following stimulation. (c) Fur loss condition in female rat. (d) Fur loss condition in male rat.

10991263, 0, Downloaded from https://analyticalsciencejournals.onlinelibrary.wiley.com/doi/10.1002/jat.4868 by China University Of Mining, Wiley Online Library on [29/07/2025]. See the Terms and Conditions (https://onlinelibrary.wiley.com/terms-and-conditions) on Wiley Online Library for rules of use; OA articles are governed by the applicable Creative Commons License

noted in the medium and high-dose groups. These symptoms were primarily observed in female rats, with less or no fur loss in males, as shown in Figure 4c,d. In the high-dose group, weak respiration was observed during the initial phase of oral exposure. Rapid breathing occurred in the low and medium-dose groups, followed by gradual improvement. Recovery time increased with concentration levels. Changes in eyelids and convulsions were not evident.

3.3 | Toxic Effects of Trans-C_6F_{12} on Samples

3.3.1 | Blood Cell Analysis

To evaluate the effects of trans-C_6F_{12} on rats, blood samples were collected on Day 14 for hematological analysis. Table 3 presents the results of hematological analysis in rats gavaged with 0, 250, 500, and 750 mg/kg of trans-C_6F_{12} on Day 14. Comprehensive hematological analyses were performed on all surviving rats at the experimental endpoint, to ensure maximal data reliability and statistical power. The final analysis included 10 control (0 mg/kg), 10 low dose (250 mg/kg), 7 medium dose (500 mg/kg), and 4 high dose (750 mg/kg) animals. Hematological analysis revealed that the low-dose group exhibited minimal alterations after oral gavage exposure. In contrast, the medium- and high-dose groups showed a significant increase in neutrophil count, a marked reduction in lymphocyte count, and an upward trend in monocyte count. Neutrophilia is a sign of acute inflammation, indicating an immune response triggered by chemical toxicants. The marked reduction in lymphocyte count may be associated with stress or immunosuppression. Meanwhile, the observed lymphocytic infiltration in histopathology reflects a dynamic immunoregulatory process: The immune system becomes activated upon tissue damage, infection, or abnormal proliferation, recruiting lymphocytes to the affected site with consequent localized infiltration. The observed upward trend in monocyte count may reflect the initiation of chronic inflammatory responses. Moreover, a significant elevation in platelet count was observed across all treatment groups. However, no statistically significant differences were detected in white blood cell or red blood cell count between groups.

3.3.2 | Toxic Effects on the Organs

The experimental results showed that oral gavage with a 250 mg/kg solution for 14 days did not cause rat mortality. However, gavage with 500 and 750 mg/kg solutions led to deaths, with higher concentrations resulting in more fatalities. To further investigate the effects of trans-C_6F_{12} on the organs of rats, histopathological analysis of tissue sections (liver, heart, spleen, lungs, kidneys, classical hippocampus, and eyes) revealed the following findings:

Figure 5 shows the pathological sections of the liver after gavage exposure. Compared with the control group, the liver tissue in the low-dose group has a capsule composed of dense connective tissue rich in elastic fibers with uniform thickness. Mild hydropic degeneration of hepatocytes (black arrow) is widely observed around the central vein, portal area, and hepatic parenchyma. The cytoplasm appears loose and pale. Occasional hepatocyte necrosis (red arrow) is observed in the hepatic parenchyma. This is accompanied by a small amount of lymphocyte infiltration (blue arrow) in the surrounding area. No significant abnormalities are observed in the liver tissue of the medium-dose group. In the high-dose group, the liver tissue capsule structure is normal. Mild hydropic degeneration of hepatocytes (black arrow) is widely observed around the central vein, portal area, and hepatic parenchyma. The cytoplasm appears loose and pale. However, no significant inflammatory cell infiltration is observed.

Overall, trans-C_6F_{12} induces mild hydropic degeneration and focal necrosis in the liver tissue of rats. It does not cause severe structural or inflammatory damage. This indicates that its toxic effect on the liver is moderate.

Figure 6 presents the pathological sections of the heart after gavage exposure. Compared with the control group, the heart tissue in the low-dose group shows small areas of irregular arrangement of myocardial cells. Occasional necrosis of myocardial cells (red arrow) is observed. There is mild proliferation of surrounding connective tissue. This is accompanied by a small amount of lymphocyte infiltration (blue arrow). No significant abnormalities are observed in the heart tissue of the medium-dose group. In the high-dose group, small areas of the

TABLE 3 | Hematological analysis of rats after trans-C_6F_{12} gavage exposure.

Item	Control group	Low dose (250 mg/kg)	Medium dose (500 mg/kg)	High dose (750 mg/kg)
White blood cell count (10^9/L)	8.68 ± 1.94	9.66 ± 1.80	7.95 ± 2.64	8.27 ± 2.57
Neutrophil count (10^9/L)	1.15 ± 0.40	1.94 ± 1.30	2.39 ± 1.27*	2.53 ± 1.24*
Lymphocyte count (10^9/L)	7.04 ± 1.66	7.08 ± 1.37	4.70 ± 1.44*	5.09 ± 1.04*
Monocyte count (10^9/L)	0.43 ± 0.19	0.57 ± 0.29	0.77 ± 0.38*	0.57 ± 0.44
Red blood cell count (10^{12}/L)	6.83 ± 0.86	7.03 ± 0.60	6.33 ± 0.28	6.30 ± 0.43
Platelet count (%)	544.50 ± 243.13	743.30 ± 142.11*	954.43 ± 161.16*	1108.00 ± 70.97*
Hemoglobin (g/L)	146.40 ± 17.26	148.90 ± 6.40	135.57 ± 5.56	139.50 ± 4.43
Hematocrit (%)	35.94 ± 5.04	37.26 ± 2.58	34.41 ± 1.39	35.03 ± 0.74

*Compared with the control group, $p < 0.05$.

10991263, 0, Downloaded from https://analyticalsciencejournals.onlinelibrary.wiley.com/doi/10.1002/jat.4868 by China University Of Mining, Wiley Online Library on [29/07/2025]. See the Terms and Conditions (https://onlinelibrary.wiley.com/terms-and-conditions) on Wiley Online Library for rules of use; OA articles are governed by the applicable Creative Commons License

epicardium show a small amount of lymphocyte infiltration (blue arrow). The surrounding myocardial cells are irregularly arranged, and the intercellular space is widened.

Overall, the damage to the heart tissue of rats caused by trans-C_6F_{12} is moderate. It is mainly characterized by local disorganization of myocardial cells, mild necrosis, and lymphocyte infiltration. It does not cause extensive or severe structural damage to the heart.

Figure 7 shows the pathological sections of the spleen after gavage exposure. Compared with the control group, the spleen tissue in the low-dose group has a capsule composed of dense connective tissue rich in elastic fibers and smooth muscle fibers with uniform thickness. The capsular connective tissue extends into the spleen to form trabeculae, with no significant abnormalities. The splenic parenchyma consists of red pulp and white pulp, with abundant white pulp of irregular shape. The boundary between red pulp and white pulp is clear, composed of splenic cords and sinusoids. A small amount of granulocyte infiltration (blue arrow) and a small amount of brown-yellow pigment deposition (orange arrow) are observed. The spleen tissue structure in the medium-dose group is similar to that in the low-dose group. However, occasional necrotic cell fragments (black arrow) are observed in the white pulp, indicating local cellular damage. The pathological changes in the spleen tissue of the high-dose group are consistent with those in the low-dose group. These include a small amount of granulocyte infiltration (blue arrow) and brown-yellow pigment deposition (orange arrow). No significant necrosis or other severe damage is observed.

Overall, trans-C_6F_{12} exerted moderate toxic effects on rat splenic tissue. It is primarily characterized by mild inflammatory responses (granulocyte infiltration) and possible deposition of metabolic products (brown-yellow pigments). The medium doses may induce localized cellular damage.

Figure 8 demonstrates the pathological sections of the lung after gavage exposure. Compared with the control group, the lung tissue in the low-dose group shows extensive hemorrhage (yellow arrow). A large number of red blood cells are observed in the alveolar cavities and bronchiolar lumens. Rare eosinophilic deposits (green arrow) are seen in the alveolar cavities. Occasional granulocyte infiltration (blue arrow) is observed in the alveolar walls. Rare necrotic cell fragments (black arrow) are found in the bronchiolar lumens. This is accompanied by a small amount of brown-yellow pigment deposition (orange arrow). In the medium-dose group, a small amount of granulocyte infiltration (blue arrow) is observed in the alveolar walls. There is mild to moderate thickening of the alveolar walls and widening of the alveolar septa. Rare necrotic cell fragments (black arrow) are found in the bronchiolar lumens. This is accompanied by mild hemorrhage (yellow arrow). In the high-dose group, a small amount of granulocyte infiltration (blue arrow) is observed in the alveolar walls. There is mild thickening of the alveolar walls and widening of the alveolar septa. Rare necrotic cell fragments (black arrow) are found in the bronchiolar lumens.

In summary, significant pathological changes are observed in the lung tissue after gavage exposure. These include hemorrhage, inflammatory cell infiltration, thickening of the

FIGURE 5 | Liver pathological sections.

FIGURE 6 | Heart pathological sections.

FIGURE 7 | Spleen pathological sections.

10991263, 0, Downloaded from https://analyticalsciencejournals.onlinelibrary.wiley.com/doi/10.1002/jat.4868 by China University Of Mining, Wiley Online Library on [29/07/2025]. See the Terms and Conditions (https://onlinelibrary.wiley.com/terms-and-conditions) on Wiley Online Library for rules of use; OA articles are governed by the applicable Creative Commons License

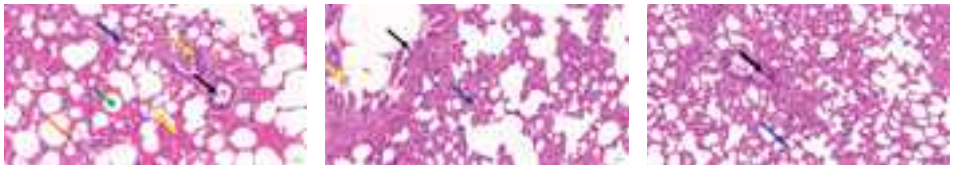

FIGURE 8 | Lung pathological sections.

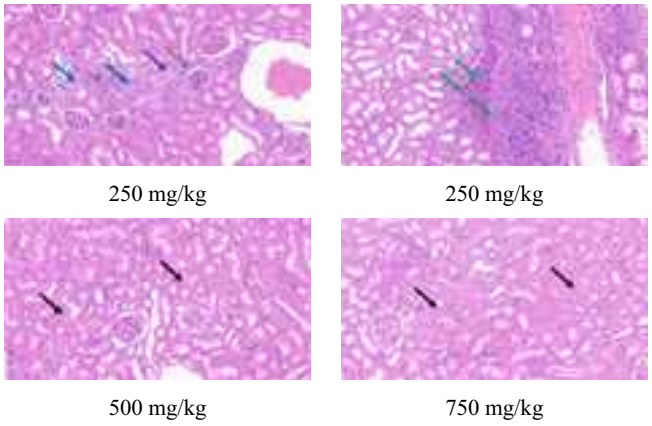

FIGURE 9 | Kidney pathological sections.

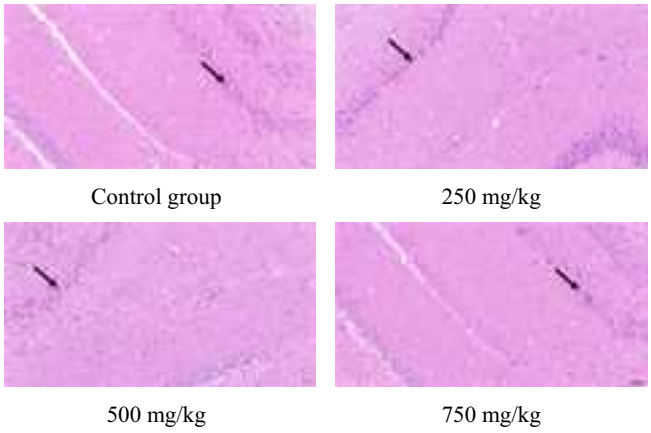

FIGURE 10 | Classical hippocampus pathological sections.

alveolar walls, and cellular necrosis. This indicates that the exogenous substance has caused severe toxic damage to the lungs. Similarly, previous studies have concluded that residents living near HF production facilities frequently exhibit symptoms of pulmonary damage and fluoride toxicity (Johnston and Strobel 2020). Fluoride may induce pulmonary oxidative stress, evidenced by elevated reactive oxygen species and proinflammatory cytokines in fluoride-exposed murine lungs (Zuo et al. 2018).

Figure 9 displays the pathological sections of the kidney after gavage exposure. Compared with the control group, the kidney tissue in the low-dose group has a capsule composed of dense connective tissue with uniform thickness. The renal parenchyma consists of the superficial cortex and deep medulla, with a clear boundary between the cortex and medulla. Small areas of interstitial connective tissue hyperplasia are observed in the cortex, accompanied by a small amount of lymphocyte infiltration (blue arrow). Rare renal tubular atrophy (purple arrow) and mild thickening of the Bowman's capsule wall (gray arrow) are seen. Severe epithelial cell hyperplasia is observed in the renal calyces of the medulla, with extensive granulocyte infiltration (green arrow) in the epithelium and calyceal cavities. There is hyperplasia of surrounding connective tissue. The kidney tissue structure in the medium-dose group is similar to that of the control group. The glomeruli in the cortex are evenly distributed, with uniform cell numbers and matrix. However, a small amount of renal tubular epithelial cell degeneration (black arrow) is observed, with loose and lightly stained cytoplasm. The pathological changes in kidney tissue of the high-dose group were consistent with those in the medium-dose group, including a small amount of renal tubular epithelial cell degeneration (black arrow).

In summary, significant pathological changes were observed in kidney tissues after exposure, including interstitial connective tissue hyperplasia, lymphocyte infiltration, renal tubular atrophy, and thickening of Bowman's capsule walls. Additionally, severe epithelial cell hyperplasia and extensive granulocyte infiltration in the renal calyces of the medulla further indicate severe inflammatory and structural damage to the kidneys. Consistent with previous findings, fluoride has been demonstrated to induce potential chronic renal toxicity (Johnston and Strobel 2020). The primary reason is that after fluoride is absorbed, it circulates through the bloodstream and is subsequently filtered by the kidneys and excreted in urine. Approximately 45%–60% of ingested fluoride is eliminated via urinary excretion (Preedy 2015), as the kidneys play a crucial role in fluoride filtration (Gerster et al. 1983; Krishnamachari 1986; Bansal and Tiwari 2006).

Figure 10 presents the pathological sections of the classical hippocampus after gavage exposure. The control group exhibited minimal pyramidal cell shrinkage (black arrows) in the hippocampal CA1 region. In contrast, shrinkage of pyramidal cells and granule cells (black arrow) is observed in the CA1, CA2, CA3, and DG regions of the hippocampus in low-, medium-, and high-dose groups. The cells exhibit deepened staining and unclear boundaries between the nucleus and cytoplasm. However, no significant necrosis, glial cell hyperplasia, or inflammatory cell infiltration is observed.

Overall, the toxic effects of trans-C_6F_{12} on the classical hippocampus of rats are primarily manifested as shrinkage and deepened staining of pyramidal cells and granule cells. This suggests that the cells may have undergone mild damage or metabolic abnormalities, but it does not induce significant necrosis, inflammation, or glial cell reactions, indicating that

10991263, 0, Downloaded from https://analyticalsciencejournals.onlinelibrary.wiley.com/doi/10.1002/jat.4868 by China University Of Mining, Wiley Online Library on [29/07/2025]. See the Terms and Conditions (https://onlinelibrary.wiley.com/terms-and-conditions) on Wiley Online Library for rules of use; OA articles are governed by the applicable Creative Commons License

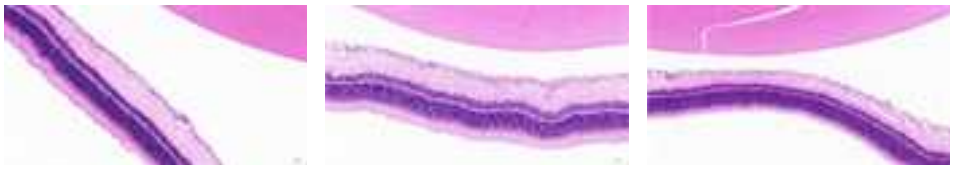

FIGURE 11 | Eyeball pathological sections.

the toxic effects of trans-C_6F_{12} on the classical hippocampus are relatively mild.

Figure 11 shows the pathological sections of the eyeball after gavage exposure. The retinal structure is clear, with the following layers visible from the inside to the outside: the internal limiting membrane, nerve fiber layer, lamina ganglionaris, inner plexiform layer, internal granular layer, external plexiform layer, external granular layer, retinal rod and cone layer, and pigment epithelial layer. The layers are tightly arranged, with clear boundaries and normal cell morphology. No significant inflammatory cell infiltration is observed. Under these conditions, trans-C_6F_{12} does not cause damage to the ocular tissue of rats.

To sum up, trans-C_6F_{12} causes severe damage to the lung and kidney tissues of rats. Its effects on the liver, heart, and spleen are moderate. The effects on the classical hippocampus are mild. No damage is observed in the ocular tissue. Therefore, trans-C_6F_{12} at concentrations of 250, 500, and 750 mg/kg primarily causes damage to the respiratory and urinary systems of rats. Researchers and fire rescue personnel must take appropriate protective measures to avoid ingestion or excessive contact with trans-C_6F_{12}.

3.3.3 | Levels of Proinflammatory Cytokines

Interleukin-1β (IL-1β) is a potent proinflammatory cytokine that plays a pivotal role in host defense responses to infection and injury. IL-1β is primarily secreted by monocytes and macrophages (Lopez-Castejon and Brough 2011). In addition, extensive literature confirms that IL-1β is a key initiator of inflammatory responses and is highly associated with fluoride toxicity (Hosokawa et al. 2011; Guo et al. 2024; Y. Zhang et al. 2020; Y. Wang et al. 2023; Y. Tian et al. 2016; Yan et al. 2016; Q. Luo et al. 2017). Thus, IL-1β serves as a sensitive and mechanistically relevant biomarker for assessing trans-C_6F_{12}-induced inflammatory toxicity. To comprehensively assess the immune and inflammatory responses triggered by toxins and reveal the pathogenic mechanisms, further IL-1β analysis was conducted on rat organ tissue sections. Furthermore, quantitative statistical analysis of fluorescence expression was performed to determine IL-1β levels, with the results shown in Figure 12.

The results of the study indicate significant differences in the toxic responses of various tissues to trans-C_6F_{12}. The liver, heart, spleen, and classical hippocampus exhibited similar response trends, with a mild increase in IL-1β levels, but the overall degree of inflammation remained relatively mild, suggesting that these tissues have a certain tolerance to trans-C_6F_{12}. In contrast, the lung and kidney tissues showed stronger responses

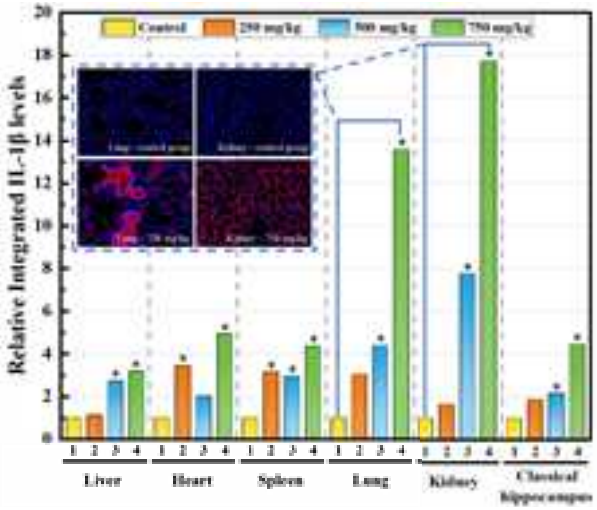

*: Compared with the control group, $P< 0.05$

FIGURE 12 | IL-1β levels analysis. *Compared with the control group, $p < 0.05$.

to trans-C_6F_{12}, with IL-1β levels significantly increasing as the exposure concentration rose, indicating that these two tissues are more sensitive to trans-C_6F_{12}.

In summary, this study reveals significant differences in the inflammatory responses of different tissues to trans-C_6F_{12} toxicity exposure. The lungs and kidneys exhibited stronger inflammatory responses, whereas the other tissues demonstrated tolerance. These findings provide important experimental evidence for further exploring the effects of trans-C_6F_{12} toxicity exposure on different organs. They also lay a theoretical foundation for subsequent toxicity assessments and the development of intervention strategies.

4 | Conclusion

This study comprehensively investigated the acute oral toxicity of trans-C_6F_{12}, a byproduct present in the $C_6F_{12}O$ fire extinguishing agent, through a series of experiments on rats. The experimental design comprised four treatment groups: control group, low-dose (250 mg/kg), medium-dose (500 mg/kg), and high-dose (750 mg/kg) groups, covering the range from sublethal to lethal concentrations. The findings provide critical insights into the toxicological effects of trans-C_6F_{12}, particularly its impact on vital organs and systemic responses. The key conclusions are as follows:

1. The sex-specific LD50 values were determined to be 823 mg/kg for female rats and 558 mg/kg for male rats, with

10991263, 0, Downloaded from https://analyticalsciencejournals.onlinelibrary.wiley.com/doi/10.1002/jat.4868 by China University Of Mining, Wiley Online Library on [29/07/2025]. See the Terms and Conditions (https://onlinelibrary.wiley.com/terms-and-conditions) on Wiley Online Library for rules of use; OA articles are governed by the applicable Creative Commons License

a combined LD50 of 655 mg/kg when sex differences were not considered. This indicates mild acute toxicity. Clinical observations revealed dose-dependent effects, including lethargy, reduced food and water intake, weight loss, and gastrointestinal disturbances such as watery feces.

2. Pathological analysis showed that trans-C_6F_{12} primarily affects the respiratory and urinary systems. It caused significant damage to lung and kidney tissues. In contrast, its effects on the liver, heart, and spleen are moderate. The effects on the classical hippocampus are mild. No damage was observed in ocular tissues.

3. Analysis of the proinflammatory cytokine IL-1β levels further evaluated the effects of trans-C_6F_{12} on inflammatory responses and the immune system in various organs. The results showed that the lungs and kidneys exhibited significant inflammatory responses, with IL-1β levels significantly increasing with dose escalation. In contrast, the liver, heart, spleen, and classical hippocampus exhibited an aggravating trend in IL-1β levels, indicating relatively mild inflammatory responses. These findings suggest that the lungs and kidneys are more sensitive to the toxicity of trans-C_6F_{12}.

4. During fire suppression operations, firefighters must wear complete protective clothing, always operate upwind, and maintain a certain discharge distance to reduce exposure to trans-C_6F_{12}. Additionally, regular medical monitoring should be conducted, with emphasis on pulmonary and renal function examinations.

In conclusion, this study elucidates the toxicological profile of trans-C_6F_{12} and highlights its potential risks to human health. The findings contribute to a better understanding of the safety implications of using $C_6F_{12}O$ fire extinguishing agent and lay a foundation for developing effective protective measures and regulatory guidelines.

Acknowledgments

This work is supported by the Beijing Municipal Science and Technology Project (Z231100003823022), the Ordos Key Research and Development Program (No. YF20240026), the Beijing Nova Program (No. 202504841008), Tianjin Natural Science Foundation Project (22JCZDJC00880), Key-Area Research and Development Program of Guangdong Province (2024B1111080002), and the Fundamental Research Funds for the Central Universities (No. 2025ZKPYAQ03).

Conflicts of Interest

The authors declare no conflicts of interest.

Data Availability Statement

The data that support the findings of this study are available from the corresponding author upon reasonable request.

References

Babushok, V. I., V. R. Katta, and F. Takahashi. 2022. "Equivalence Ratio Influence on the Flame Suppressant Concentration of 2-BTP and Novec 1230." *Combustion Science and Technology* 194, no. 10: 1943–1953.

Bansal, R., and S. C. Tiwari. 2006. "Back Pain in Chronic Renal Failure." *Nephrology, Dialysis, Transplantation* 21, no. 8: 2331–2332.

Cui, J., S. Yan, S. Bi, and J. Wu. 2018. "Saturated Liquid Dynamic Viscosity and Surface Tension of Trans-1-Chloro-3, 3, 3-Trifluoropropene and Dodecafluoro-2-Methylpentan-3-One." *Journal of Chemical and Engineering Data* 63, no. 3: 751–756.

Fan, R., Y. Pan, X. Shi, Y. Lu, and Z. Wang. 2023. "Investigation on the Suppression Effect of High Momentum C6F12O (Novec-1230) Flow on Hydrogen Jet Flame." *Journal of Loss Prevention in the Process Industries* 84: 105128.

Gerster, J., S. Charhon, P. Jaeger, et al. 1983. "Bilateral Fractures of Femoral Neck in Patients With Moderate Renal Failure Receiving Fluoride for Spinal Osteoporosis." *BMJ (Clinical Research Edition)* 287, no. 6394: 723–725.

Guo, H.-W., X.-P. Wang, W.-P. Zhao, J. Zhao, H.-W. Li, and M. Zheng. 2024. "Effect of Fluoride on the Expression of Th17-Related Cytokines Profiles in Hepa1–6 Cells."

Han, Z., X. Zhang, Y. Yu, et al. 2023. "Experimental Investigation of Fire Extinguishing of a Full-Size Battery Box With FK-5-1-12." *Fire Technology* 59, no. 3: 1269–1282.

Han, Z., R. Zi, Y. Yu, Z. Du, L. Liu, and L. Deng. 2023. "Study on the Minimum Extinguishing Concentration of C6F12O for Extinguishing Synthesis Gas Flame of Lithium-Ion Battery." *Journal of Thermal Analysis and Calorimetry* 148, no. 9: 3631–3643.

Hosokawa, M., Y. Inoue, X.-F. Chen, et al. 2011. "The Alterations in Cytokine mRNA Expressions and Productions by Fluoride in a Murine Macrophage Cell Line Evaluated by Real-Time PCR and ELISA." *Biomedical Research on Trace Elements* 22, no. 1: 27–33.

Huang, J., J. Jin, J. Liang, Y. He, and Y. Chen. 2025. "Experimental Study on Fire Suppression of NCM Lithium-Ion Battery by C6F12O in a Confined Space." *Applied Thermal Engineering* 259: 124932.

Johnston, N. R., and S. A. Strobel. 2020. "Principles of Fluoride Toxicity and the Cellular Response: A Review." *Archives of Toxicology* 94, no. 4: 1051–1069.

Krishnamachari, K. 1986. "Skeletal Fluorosis in Humans: A Review of Recent Progress in the Understanding of the Disease." *Progress in Food and Nutrition Science* 10, no. 3–4: 279–314.

Li, Y., X. Zhang, S. Tian, S. Xiao, Y. Li, and D. Chen. 2019. "Insight Into the Decomposition Mechanism of C6F12O-CO2 Gas Mixture." *Chemical Engineering Journal* 360: 929–940.

Liu, L., Z. Du, T. Zhang, Z. Guo, M. He, and Z. Liu. 2019. "The Inhibition/Promotion Effect of C6F12O Added to a Lithium-Ion Cell Syngas Premixed Flame." *International Journal of Hydrogen Energy* 44, no. 39: 22282–22300.

Lopez-Castejon, G., and D. Brough. 2011. "Understanding the Mechanism of IL-1β Secretion." *Cytokine and Growth Factor Reviews* 22, no. 4: 189–195.

Luo, N., H. Mi, X. Wang, et al. 2025. "Combustion Inhibition and Promotion Mechanisms of C3F7COC2F5 in H_2-CH_4-Air Mixture Flames." *Process Safety and Environmental Protection* 201: 107392.

Luo, Q., H. Cui, H. Deng, et al. 2017. "Sodium Fluoride Induces Renal Inflammatory Responses by Activating NF-κB Signaling Pathway and Reducing Anti-Inflammatory Cytokine Expression in Mice." *Oncotarget* 8, no. 46: 80192–80207.

McLinden, M. O., R. A. Perkins, E. W. Lemmon, and T. J. Fortin. 2015. "Thermodynamic Properties of 1, 1, 1, 2, 2, 4, 5, 5, 5-Nonafluoro-4 -(Trifluoromethyl)-3-Pentanone: Vapor Pressure, (p, ρ, T) Behavior, and Speed of Sound Measurements, and an Equation of State." *Journal of Chemical and Engineering Data* 60, no. 12: 3646–3659.

OECD. 2001. "Test No. 423: Acute Oral toxicity—Acute Toxic Class Method."

10991263, 0, Downloaded from https://analyticalsciencejournals.onlinelibrary.wiley.com/doi/10.1002/jat.4868 by China University Of Mining, Wiley Online Library on [29/07/2025]. See the Terms and Conditions (https://onlinelibrary.wiley.com/terms-and-conditions) on Wiley Online Library for rules of use; OA articles are governed by the applicable Creative Commons License

Pagliaro, J. L., and G. T. Linteris. 2017. "Hydrocarbon Flame Inhibition by C6F12O (Novec 1230): Unstretched Burning Velocity Measurements and Predictions." *Fire Safety Journal* 87: 10–17.

Pan, C., J. Zhao, X. Zhu, et al. 2021. "Synergy Effects of Novec 1230 and Venting on Ethanol-Gasoline Vapor Explosion Inhibition." *Energy Sources, Part A: Recovery, Utilization, and Environmental Effects*: 1–19.

Perkins, R. A., M. L. Huber, and M. J. Assael. 2018. "Measurement and Correlation of the Thermal Conductivity of 1, 1, 1, 2, 2, 4, 5, 5, 5-No nafluoro-4-(Trifluoromethyl)-3-Pentanone." *Journal of Chemical and Engineering Data* 63, no. 8: 2783–2789.

Preedy, V. R. 2015. *Fluorine: Chemistry, Analysis, Function and Effects*. Cambridge: Royal Society of Chemistry.

Tian, S. S., Z. Li, C. Y. Li, and X. X. Zhang. 2024. "Study on the Inhibition Effect of C6F12O on Charged Particles in the Flame of Transformer Oil Discharge Gas." *Combustion Science and Technology* 197: 1–20.

Tian, Y., M. Huo, G. Li, Y. Li, and J. Wang. 2016. "Regulation of LPS-Induced mRNA Expression of Pro-Inflammatory Cytokines via Alteration of NF-κB Activity in Mouse Peritoneal Macrophages Exposed to Fluoride." *Chemosphere* 161: 89–95.

Wallig, M. A., B. Bolon, W. M. Haschek, and C. G. Rousseaux. 2017. *Fundamentals of Toxicologic Pathology*. Academic Press.

Wang, J., B. Chen, Q. Li, et al. 2025. "Inhibition Effect and Kinetics Studies on the Deflagration Characteristics of Hydrogen Compressed Natural Gas (HCNG) by C6F12O and CO2." *International Journal of Hydrogen Energy* 113: 523–534.

Wang, K., D. Ouyang, S. Yuan, et al. 2025. "Experimental Study on Inhibition Effect of Novec-1230 on Thermal Runaway Fire of Lithium-Ion Battery Packs Induced by Overcharging." *Journal of Energy Storage* 120: 116451.

Wang, X., Q. Ji, and X. Zhang. 2023. "Decomposition Kinetics of Perfluoro-(4-Methyl-2-Pentene)(C6F12) and Its Extinguishing Performance Study." *ChemistrySelect* 8, no. 43: e202303193.

Wang, Y., J. Xu, H. Chen, et al. 2023. "Effects of Prolonged Fluoride Exposure on Innate Immunity, Intestinal Mechanical, and Immune Barriers in Mice." *Research in Veterinary Science* 164: 105019.

Wen, C., X. Meng, M. L. Huber, and J. Wu. 2017. "Measurement and Correlation of the Viscosity of 1, 1, 1, 2, 2, 4, 5, 5, 5-Nonafluoro-4-(Trif luoromethyl)-3-Pentanone." *Journal of Chemical and Engineering Data* 62, no. 10: 3603–3609.

Xing, H., Y. Cheng, S. Lu, N. Tao, and H. Zhang. 2021. "A Reactive Molecular Dynamics Study of the Pyrolysis Mechanism of C6F12O." *Molecular Physics* 119, no. 24: e1976425.

Xing, H., S. Lu, J. Tao, Y. Zhou, J. Zhao, and H. Zhang. 2025. "Insight Into C6F12O Fire Suppression Mechanism on Coaxial n-Heptane Flame: Combined Experimental and ReaxFF Molecular Dynamics Simulation." *Process Safety and Environmental Protection* 200: 107383.

Xing, H., S. Lu, H. Yang, and H. Zhang. 2022. "Review on Research Progress of C6F12O as a Fire Extinguishing Agent." *Fire* 5, no. 2: 50.

Yan, N., Y. Liu, S. Liu, et al. 2016. "Fluoride-Induced Neuron Apoptosis and Expressions of Inflammatory Factors by Activating Microglia in Rat Brain." *Molecular Neurobiology* 53: 4449–4460.

Zeng, F., Z. Lei, Y. Miao, Q. Yao, and J. Tang. 2019. "Reaction Thermodynamics of Overthermal Decomposition of C6F12O." Paper presented at: The International Symposium on High Voltage Engineering.

Zhang, X., Y. Li, S. Xiao, J. Tang, S. Tian, and Z. Deng. 2017. "Decomposition Mechanism of C5F10O: An Environmentally Friendly Insulation Medium." *Environmental Science and Technology* 51, no. 17: 10127–10136.

Zhang, X., S. Tian, S. Xiao, Z. Deng, Y. Li, and J. Tang. 2017. "Insulation Strength and Decomposition Characteristics of a C6F12O and N2 Gas Mixture." *Energies* 10, no. 8: 1170.

Zhang, Y., B.-h. Zhou, P.-p. Tan, Y. Chen, C.-y. Miao, and H.-w. Wang. 2020. "Key Role of Pro-Inflammatory Cytokines in the Toxic Effect of Fluoride on Hepa1-6 Cells." *Biological Trace Element Research* 197: 115–122.

Zuo, H., L. Chen, M. Kong, et al. 2018. "Toxic Effects of Fluoride on Organisms." *Life Sciences* 198: 18–24.

10991263, 0, Downloaded from https://analyticalsciencejournals.onlinelibrary.wiley.com/doi/10.1002/jat.4868 by China University Of Mining, Wiley Online Library on [29/07/2025]. See the Terms and Conditions (https://onlinelibrary.wiley.com/terms-and-conditions) on Wiley Online Library for rules of use; OA articles are governed by the applicable Creative Commons License